Effect of interface chemistry on charge injection and trapping in polyethylene blend

Somyot **TANTIPATTARAKUL**, Alun S. **VAUGHAN**, Thomas **ANDRITSCH,** Suvi **VIRTANEN;** the University of Southampton, (United Kingdom),
st2f14@soton.ac.uk, asv@ecs.soton.ac.uk, T.Andritsch@soton.ac.uk, S.Virtanen@soton.ac.uk

ABSTRACT

The electrical characteristics of dielectric surfaces are important in determining overall electrical performance. In this work, one surface of polyethylene blend films was treated at a high temperature for various times to modify the local chemistry. Confocal Raman microprobe spectroscopy was subsequently employed to detect signatures of ageing at the surface and through bulk of specimens. The pulsed electro-acoustic (PEA) method was used to investigate charge injection and trapping processes. The results demonstrate that chemical changes resulting from ageing cause dramatic and abrupt changes in the charge transport dynamics within the system.

KEYWORDS

Thermal treatment; surface ageing; space charge.

INTRODUCTION

There is great interest in the effects of relevant factors on charge injection and transport processes in polyethylene (PE) systems under the action of high electric fields. According to many studies [1, 2], the electronic surface properties will be related to the presence of localised surface states which, in turn, will affect carrier injection into the bulk. The surface states may have different origins depending on the physical and chemical surface structure of the PE and the electrodes, such as the surface topography, impurities and contamination. For the band structure of polymers, the surface states can lead to either the enhancement or suppression of charge injection due to the generation of the localized energy levels in the bandgap [3]. Thus, changes in injection process inevitably affect space charge (SC) accumulation in the bulk of polymers. Although many effects related to different interface conditions on the charge injection behaviours have been reported [4-6], little attention has been given to the effect of surface chemistry modification of PE that occur as a result of ageing processes.

In this paper, thermal treatment at a high temperature for varying times was used to generate thermally oxidized surface with various degrees of ageing in PE blend samples. Signatures of thermal ageing were investigated using Fourier transform infrared (FTIR) and confocal Raman spectroscopies were used to probe chemical changes; optical microscope was used to reveal changes via cross-section of the treated samples. The PEA technique was used to explore the effect of interfacial modification on charge injection and space charge accumulation

SAMPLE PREPARATION AND THERMAL TREATMENT CONDITIONS

All of specimens were produced from blends containing 20% of high-density polyethylene (HDPE; grade HD5813EA; BP Chemicals) and 80% low-density polyethylene (LDPE; grade LD100BW; Exxon Mobil), which were prepared by melt mixing in a HAAKE Polylab twin rotor R600 mixer. The blended polymer was pressed at 160 ºC for 5 mins to give thin films ~200 μm in thickness. Thereafter, the films were directly quenched into water at 20 ºC. The un-aged material was used as a reference system. Thermal ageing was performed at 160 ºC for 1 to 6 h; the treatment period between 3 and 4 h was examined with increased temporal resolution, with ageing times of 3:07 h, 3:15 h, 3:30 h and 3:45 h being considered. During the ageing process, one surface of each sample was exposed to air, while the other was in contact with a PET (Polyethylene terephthalate) films, to minimize the influence of atmospheric oxygen.

To analyze chemical changes as a function of position, cross-sections through representative samples were prepared. Since the samples were very thin, they were first sandwiched between thicker polymer sheets (KRATON G1650 supplied from Shell; 0.1 mm in thickness), which provides the mechanical integrity required for cryo-microtomy. Fig.1 illustrates the sample cutting process.
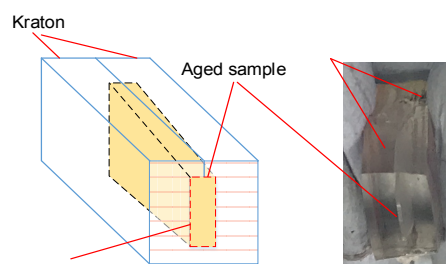

Fig. 1: The sample after cutting by cryo-microtome.

EXPERIMENTAL METHODS

Optical microscope

A Leitz Aristomet optical microscope with Leitzlar objective lenses was used to capture the micrographs of the cross-section of the treated samples; x50 objective lenses were used with the microscope operating in bright field reflection mode. Images were recorded by a Delta Pix DP3 300 CCD camera and the related software. Only a selection of significant results are shown in this paper, on grounds of brevity.

Fourier-transform infrared spectroscopy

FTIR spectroscopy was used in attenuated total reflection (ATR) mode (iD7 AR diamond crystal plates) to determine chemical modification on both surfaces of the samples after thermal treatment. Infrared spectra were obtained over the wavenumber range 500-4000 cm^{-1}; for each spectrum; 16 scans were averaged with 4 cm^{-1} resolution. To represent the degree of oxidation, the carbonyl concentration was calculated in terms of the carbonyl index [7], as follows:

$$\text{Carbonyl Index (CI)} = A_c/A_{ref} \qquad [1]$$

where A_{ref} is the area under the chosen reference bands related to CH_2 and CH_3 symmetric and asymmetric stretch (2915 and 2847 cm^{-1}); A_c is the area under the carbonyl intense peak located in the range 1720±10 cm^{-1} (C=O stretch mode).

Raman microprobe spectroscopy

Chemical analysis as a function of cross-sectional position was performed using a Renishaw RM1000 Raman microprobe system including a Renishaw NIR 780TF diode laser (wavelength 780 nm) with a maximum output power of 25 mW and an x50 objective lens, operating in confocal mode. Data were acquired from 19 measuring points equally spaced across each sample; the initial and final points were chosen to be about 10 μm from each surface of the sample, to avoid any overlapping signal generated in the surrounding KRATON sheet. This is shown schematically in Fig. 2. All spectra were acquired using 10 consecutive 10 s extended scans between 3200 cm^{-1} and 500 cm^{-1}, with the laser power set at 50%. The resulting raw spectral data were then processed using in Origin 2016, as follows. Background subtraction with first performed, after which, the peaks of interest normalized with respect to the Raman peak at 1295 cm^{-1} which is related to the C-C twisting mode, to minimize the effect on the Raman scattering intensity between each measurement (e.g. sample focusing). The carbonyl index for each measured point was again calculated according to (1), where the A_{ref} is the area under the peaks appearing at 2850 and 2883 cm^{-1} (CH_2 and CH_3 symmetric and asymmetric stretch); A_c is the area under the carbonyl peak located at 1720±5 cm^{-1} (C=O stretch mode).
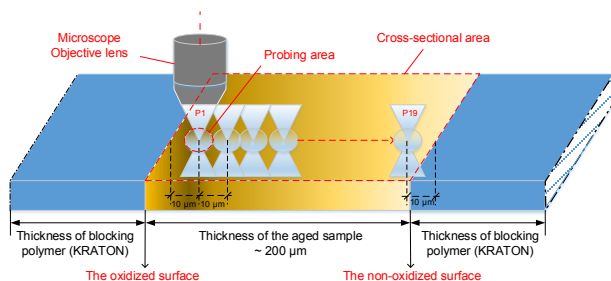

Fig. 2: Raman probing across the thickness of the sample.

Space charge measurements

Space charge measurements were performed using a PEA system. Data were acquired through the application of voltage pulses 600 V in amplitude and with a duration of 5 ns, which induce acoustic waves in the sample. The anode (high voltage electrode) and the cathode (ground) electrodes were, respectively, composed of a semiconducting polymer and aluminium. Silicone oil was used between the samples and the electrodes to obtain a good acoustic matching at each interface.The space charge dynamics were continuously investigated for 3600 s under an applied filed of +40 kV/mm (voltage-on) at room temperature. Specifically, the anode was in contact with the oxidized surface. Subsequent data processing used the calibration trace and a deconvolution technique to recover the space charge distribution in the specimen. LabVIEW software was used for the data analysis.

RESULTS

Changes in surface chemistry

The chemical modification of the surface

From Fig. 3, it is evident that significant changes in the surface chemistry occurred with treatment times of more than 2 h; specifically, infrared absorbance within the broad ranges A (~800-1500 cm^{-1}) and B (~1600-1800 cm^{-1}) are seen. The significant changes in range A are associated with the vibration bands of vinyl groups (874 and 903 cm^{-1}), ethers (1112 and 1134 cm^{-1}) and esters (1100, 1170, 1264 and 1289 cm-1). While, the changes in range B are related to carbonyl groups, such as ketone, ester and aldehyde, and γ-lactone, located at (1716, 1725 and 1780 cm^{-1}).
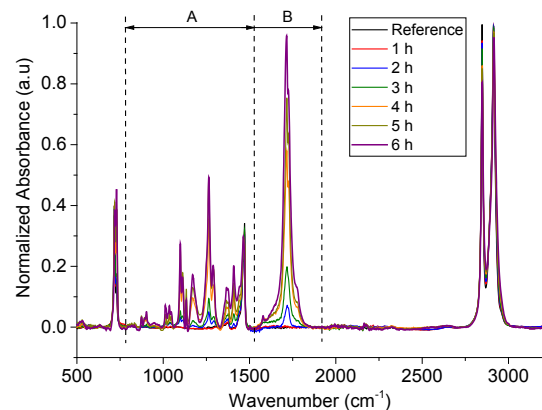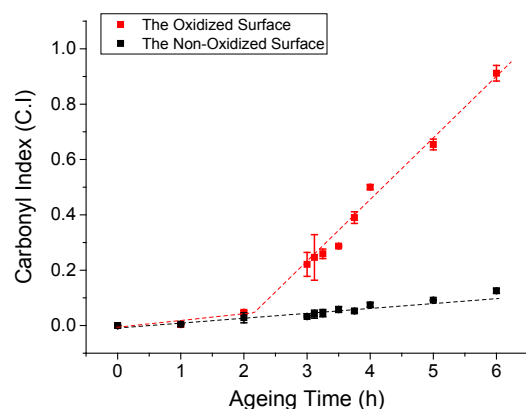

Fig. 3: FTIR spectra of samples treated for 0 h to 6 h.

Fig. 4: Carbonyl index data obtained from the oxidized and non-oxidized surface of the reference and treated samples from 0 h to 6 h.

Fig. 4 shows the variation in carbonyl index with ageing time for the oxidized and non-oxidized surfaces of the reference and treated samples from 0 h to 6 h, from which, it is evident that the carbonyl concentration at both surfaces increases with ageing time. The CI of the oxidized surface increases slightly with treatment time from 0 h to 2 h, then subsequently increases much more rapidly from 3 h to 6 h. Conversely, the CI of the surface that was not exposed to the atmosphere increases only gradually over the complete treatment time. The degree of oxidation between both surfaces is significantly different for treatments beyond 2 h. Moreover, in Fig. 5, vinyl groups were also found to be present in the oxidized surface, beyond 3 h. It is these vinyl groups that are responsible for the observed change in sample color (increased yellowing) at longer ageing times.
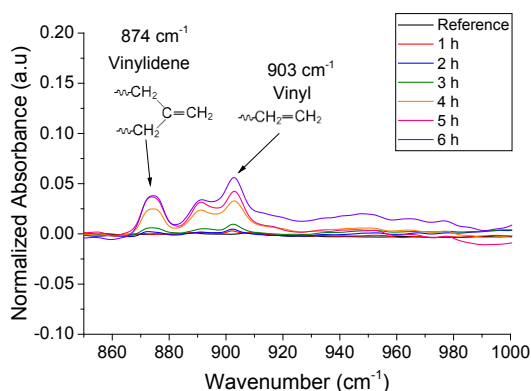

Fig. 5: The IR spectra of vinyl intense bands obtained from the oxidized surface treated from 0 h to 6 h.

Changes in bulk chemistry

Cross-sectional feature

Figs. 6(a) to 6(d) show low magnification cross-sectional images together with high magnification details for samples treated for 3 h and 6 h. In Figs. 6(a) and 6(b), the bulk feature for the sample treated for 3 h seems homogenous without any remarkable features. Whereas, many black defects (hollow forms), in Figs. 6(c) and 6(d), appeared in the sample treated for 6 h near to the oxidized surface.

(a)   (b)


(c)   (d)
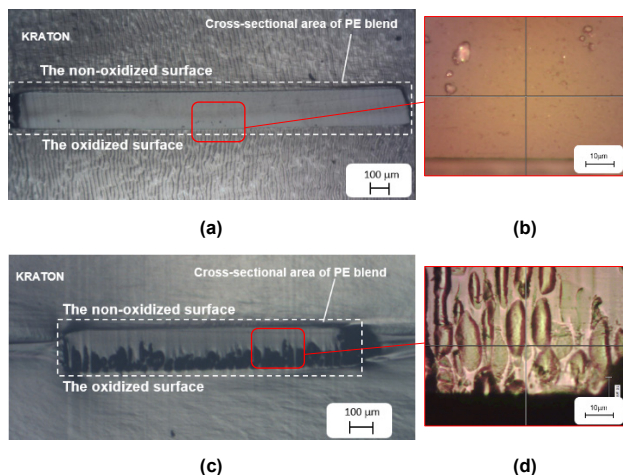
Fig. 6: The cross-sectional areas of the treated samples with the treatments for (a) 3 h and (b) 6 h.

Additionally, the bulk features for the slightly oxidized samples (1 h and 2 h) and the severely oxidized samples (4 h and 5 h) were similar to that of the samples treated for 3 h and 6 h respectively.

The chemical modification via the bulk

Fig. 7 shows the Raman spectra measured from each point across the thickness of the sample treated for 6 h. Data acquisition started from close to the upper (10 μm), oxidized surfaces and progressed to the non-oxidized surfaces (190 μm). The position affected, in particular, the intensity of three vibration bands, which are associated with primary alcohols (C-C-OH symmetric stretch; 871 cm^{-1}), vinyl groups (C=C stretch; 1618 cm^{-1}) and carbonyl groups (C=O stretch; 1720 cm^{-1}). Fig. 8 shows the change of carbonyl concentration in the bulk for samples treated for between 3 h and 6 h. CI values obtained by Raman spectroscopy were, numerically, noticeably less than those determined by FTIR due to the different physics involved. Nevertheless, the CI was found to decrease with distance from the sample's upper surface as far as ~130 μm into the bulk; thereafter, it remained constant. These two regions are considered to be oxidized and non-oxidized layers respectively. In Fig. 8, the lines representing the decrease in CI with position are either exponential or sigmoidal in form, the choice depending on the particular treatment time.
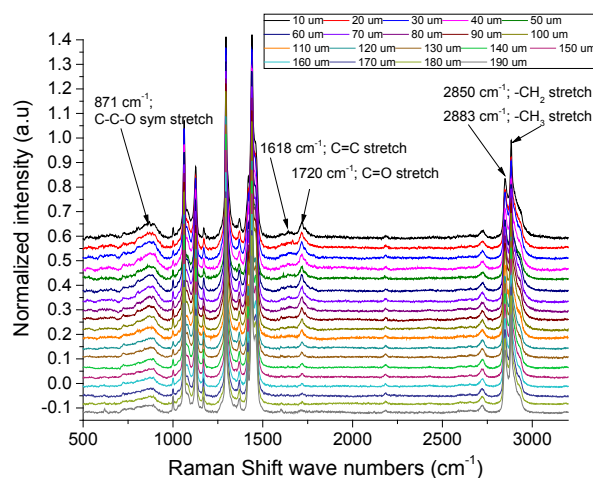

Fig. 7: Raman spectra obtained from different positions across the thickness of the sample previously treated for 6 h.
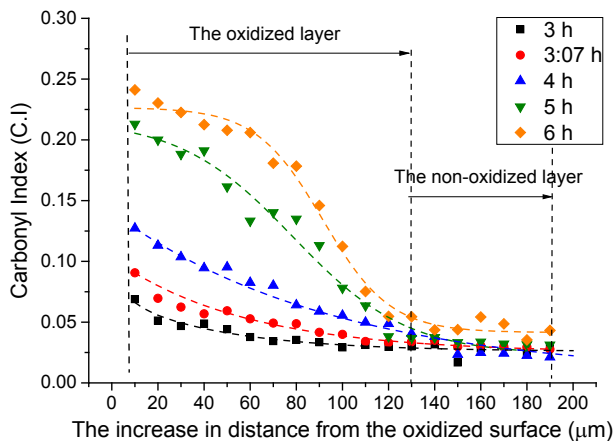
Fig. 8: Variation of carbonyl index with position for the samples treated from 3 h to 6 h.
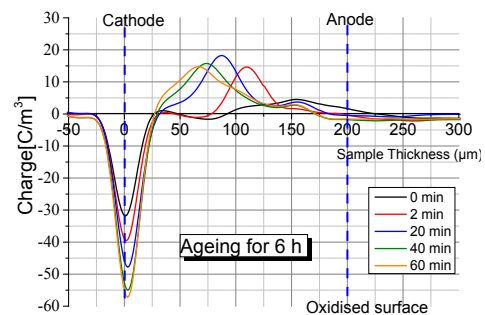
Space charge accumulation

Figs. 9(a) to 9(c) show space charge (SC) profiles obtained from the reference and thermally treated samples, where the anode was in contact with the oxidized surface. The SC results of the samples treated for 3 h and 6 h are used to represent slightly treated samples (1-3 h) and the severely treated samples (4-6 h) respectively. In Fig. 9(a), heterocharge was found in the reference sample with a significant amount of charge, rather than, negative charge, being present. In Fig. 9(b), the slightly oxidized surface caused a significant decrease in SC accumulation compare with Fig. 9(a), which heterocharge was replaced with homocharge. A radically different SC profile is evident in Fig. 9(c), where the presence of the severely oxidized surface resulted in a progressive increase in the amount of accumulated positive charge, which progressively moves from the anode into the bulk. No anode charge peak is then evident. For the samples treated for between 3 h and 4 h, the positive anode charge initially moved and became re-distributed into the bulk as shown in Fig. 13 for the sample treated for 3:07 h.
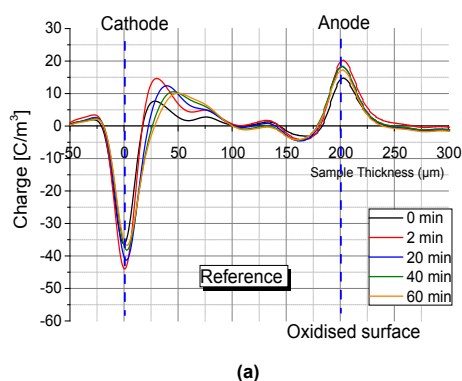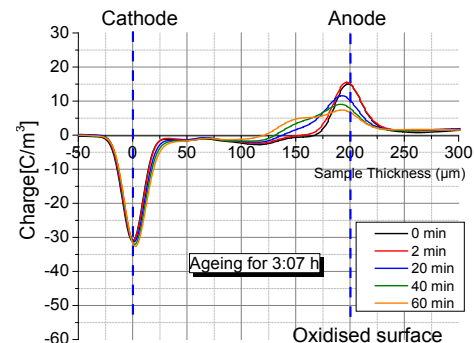

(a)
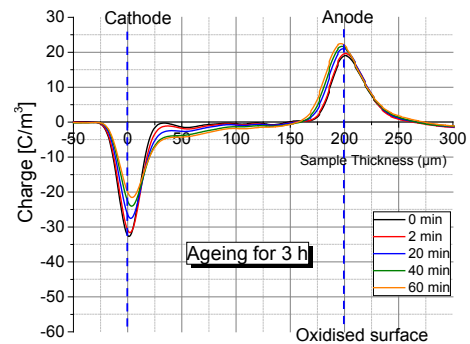
(b)

(c)

Fig. 9: Space charge accumulation in (a) the reference sample and the treated samples with the treatments for (b) 3 h and (c) 6 h.


Fig. 10: Space charge accumulation in the treated sample with the treatment for 3:07 h.

DISCUSSION

As designed, the surface in contact with air underwent major chemical changes, whereas the surface in contact with the PET substrate exhibited fewer chemical changes. From Fig. 4, the different rate of increase in the carbonyl concentration compared between both surfaces is attributed to the different availability of oxygen at each surface. In addition, the observed variation in CI on the exposed surface suggest that this region underwent induction (0-2 h) and autoxidation (2-6 h) stages of thermo-oxidative mechanism [8, 9]. These two stages depend on the C-H bonds strength, the crystallinity degree, the presence of substituents composing impurities and antioxidant. However, the accelerated increase in CI related to the autoxidation stage may rather relate to the chemical nature of PE blend than the depletion of the antioxidant, since the blend does not

include the antioxidant using for thermal stability. For bulk modification, no intrinsic defects originating from thermal ageing were observed within the cross-sectional area, as in case of the black defects detected on the oxidized surface. In Fig. 6(c) and (d), the black defects originated from deformation of the degraded material layer due to the cutting process, despite this being conducted under cryogenic (-40°C) conditions. This, we surmise, is due to the brittleness of oxidized layer of the samples treated for more than 3 h, as a consequence of thermal oxidation [8]. Indeed, from Fig. 8, the variation in CI across the thickness indicates that the aged material can be divided into two different layers, which are more and less oxidized. The former layer possess the non-uniform distribution for oxidation that arises as a result of diffusion of oxygen through the sample, where it reacts [10]. Conversely, the degree of oxidation was uniform in the latter layer, since the oxidation there mostly occurs through reaction with pre-existing oxygen rather than diffusing oxygen downwards from the exposed surface. As a result, the oxidized layer was formed from the exposed surface of the treated samples, where the degree of oxidation relies on the rate of oxygen diffusion and oxygen uptake throughout the varying treatment time.

In terms of SC accumulation, in Fig. 9(a), the origin of the heterocharge in the reference sample is associated with the specific morphology of the blend, as explained in our previous work [11]. In Figs. 9(b) and 9(c) the oxidized surface in contact with the anode clearly has a major effect on space charge accumulation in the bulk. The slightly and severely oxidized surfaces lead, respectively, to a decrease and increase in the SC accumulation. It seems that change in the surface states associated with thermal oxidation markedly influence the bulk SC behavior, with respect to injection and trapping process. In the band structure of polymers, chemical and physical defects respectively generate deep and shallow traps [12] for charge carries. The trap density therefore would be expected to increase with severity of ageing [13]. Thus, the trap density in the case of slightly and severely oxidized surfaces should have low and high trap densities respectively. This is mainly evinced by the increase in the carbonyl concentration in the oxidized layer at considerable treatment times, as shown in Fig. 8. The slightly oxidized surface, having a relatively low density of deep traps (i.e. carbonyl groups), acts as a hindrance for positive charge injection. This is because the positive charges have low possibility to hope or tunnel between traps that are well separated (D), as shown in Fig.11 (a).
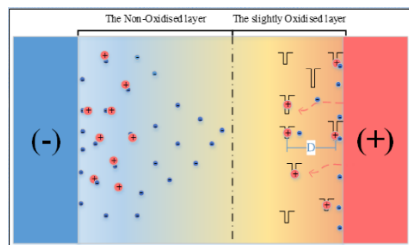
(a)
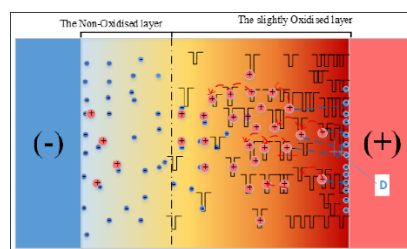
(b)

Fig. 11: The trapping schemes for injected positive charges when the anode in contact with (a) the slightly and (b) severely oxidized surfaces.

When a critical level of oxidation is reached, the oxidized surface layer may facilitate charge transport through hopping and/or tunneling processes, due to the consequent decrease in distance between neighboring traps, as shown in Fig. 11(b). Under the conditions pertinent here, the critical or threshold degree of oxidation falls close to 3 h since, beyond this ageing time the injected positive charges increase in number and progressively migrate into the bulk, as demonstrated by the SC result shown for the sample aged for 3:07 h (see Fig 10). Such enhancement of positive injection/migration increases with the degree of oxidation from 4 h to 6 h. Additionally, the peak in the accumulated positive charge distribution for 4 h, 5 h and 6 h stopped at the different distances away from the cathode (90, 78 and 70 μm respectively). It is noteworthy that these positions correspond to a similar carbonyl index value of 0.625. This implies that the oxidized layer progressively enlarges into the bulk with increased treatment time. According to our previous work [11], equivalent SC accumulation also occurs in the case when the oxidized surface is in contact with the cathode. While the correlation between CI and SC data are intriguing, this does not unambiguously demonstrate causality; alternatively, since vinyl groups appear for treatment more than 3 h, these moieties may contribute to the conduction of injected charges. In other words, the increase in the vinyl groups, which may be formed as non-conjugated and conjugated structures, may be responsible for an effective local reduction in the band gap energy of PE [14]. Nevertheless, the effect of vinyl groups on trapping process have not been clearly proved by a specific experiment.

CONCLUSION

Because of the specific method and various thermal treatments used in this study, an oxidized surface was produced on one surface of the treated samples with significant degree of oxidation compared to the other, depending on the rate of oxygen consumption. The gradient concentration of oxygen diffusing through the oxidized surface caused, in particular, the decrease in degree of oxidation from the surface into the bulk. The degree of oxidation relatively increased with increased treatment time, as represented by the carbonyl concentration. For charge injection and trapping process, the slightly (1-3 h) and severely (4-6 h) oxidized specimens are characterized by suppression and enhancement of charge injection/transport, leading to a significant decrease and increase of SC accumulation respectively. Moreover, it is noteworthy that the trapped charges at the interface between the oxidized surface and

the anode begin to hop and tunnel into the bulk at higher oxidation degrees beyond the threshold treatment time of 3 h. As a result, it is apparent that the surface ageing signatures via thermal ageing have a remarkable effect on the space charge dynamics in HDPE/LDPE polyethylene blend considered here, associated with the carrier injection and trapping processes at the modified interface. Indeed, the observed variation in space charge distribution will lead to marked variations in the electric field distribution within the system which will, in turn, modify the effective electrical performance of the PE.

REFERENCE

[1] G. Chen, Y. Tanaka, T. Takada, and L. Zhong, "Effect of Polyethylene Interface on Space Charge Formation," *IEEE Transactions on Dielectrics and Electrical Insulation,* vol. 11, pp. 113-121, 2004.

[2] C. Laurent, F. Baudoin1, V. Griseri, S. L. Roy, and G. Teyssèdre, "A discussion on the electronic properties of polyethylene interfaces," in *Proceedings of 2011 International Conference on Electrical Insulating Materials (ISEIM)*, Kyoto, Japan, 2011.

[3] M. Taleb, G. Teyssèdre, S. L. Roy, and C. Laurent, "Modeling of Charge Injection and Extraction in a Metal/Polymer Interface through an Exponential Distribution of Surface States," *IEEE Transactions on Dielectrics and Electrical Insulation* vol. 20, pp. 311-320, February 2013 2013.

[4] Z. Yuanxiang, W. Yunshan, W. Ninghua, and S. Qinghua, "Effect of surface topography and morphology on space charge packets in polyethylene," *Journal of Physics: Conference Series,* vol. 183, p. 012009, 2009.

[5] C. J. Zheng, B. Guan, H. Zhao, J. M. Yang, and Z. Sun, "Effects of Surface Morphology on Space Charge Formation in Low Density Polyethylene," *IEEE Transactions on Dielectrics and Electrical Insulation* vol. 23, 2016.

[6] Z. An, C. Xie, Y. Jiang, F. Zheng, and Y. Zhang, "Significant suppression of space charge injection into linear low density polyethylene by surface oxyfluorination," *Journal of Applied Physics,* vol. 106, pp. 1-4, 2009.

[7] ASTM, "Standard guide for evaluating the extent of oxidation in polyethylene fabricated forms intended for surgical implants," in *ASTM standard F2102-13*, ed. West Conshohocken, United States: Tech. Rep, 2013, pp. 1002-1005.

[8] A. Peacock, *Handbook of Polyethylene: Structures: Properties, and Applications*. Baytown, Texus: Marcel Dekker, Inc., 2000.

[9] F. H. Winslow, M. Y. Hellman, W. Matreyek, and S. M. Stills, "Autoxidation semicrystalline polyethylene," *Polymer Engineering & Science,* vol. 6, pp. 273-278, 1966.

[10] M. Veitmann, R. Jumeau, P. Bourson, M. Ferriol, and F. Lahure, "Understanding and Control of High Temperature Oxidation Flaws of Low-Density Poly(ethylene) with Raman Spectroscopy," *International Journal of Spectroscopy,* vol. Volume 2014, pp. 1-9, 2014.

[11] S. Tantipattarakul, A. Vaughan, and T. Andritsch, "On the effects of molecular composition, morphology and ageing on the electrical properties of polyethylene," presented at the 2016 IEEE Conference on Electrical Insulation and Dielectic Phenomena (CEIDP), Toronto, Canada, 2016.

[12] T. C. Zhou, G. Chen, R. J. Liao, and Z. Xu, "Charge trapping and detrapping in polymeric materials: trapping parameters," *Journal of Applied Physics,* vol. 110, pp. 1-6, 31 August 2011 2001.

[13] A. Tzimas, S. M. Rowland, and L. A. Dissado, "Effect of electrical and thermal stressing on charge traps in XLPE cable insulation," *IEEE Transactions on Dielectrics and Electrical Insulation,* vol. 19, pp. 2145-2154, 2012.

[14] L. Chen, T. D. Huan, and R. Ramprasad, "Electronic Structure of Polyethylene: Role of Chemical, Morphological and Interfacial Complexity," 21 July 2017 2017.